Brillouin scattering in molten and crystalline alkali halides

S. L. Qiu
Department of Physics, City College of the City University of New York, New York, New York 10031

R. A. J. Bunten
Clarendon Laboratory, University of Oxford, Parks Road, Oxford OX1 3PU, United Kingdom

M. Dutta
Department of Physics, City College of the City University of New York, New York, New York 10031

E. W. J. Mitchell
Clarendon Laboratory, University of Oxford, Parks Road, Oxford OX1 3PU, United Kingdom

H. Z. Cummins
Department of Physics, City College of the City University of New York, New York, New York 10031
(Received 30 August 1984)

Brillouin scattering experiments were performed on molten CsCl and on molten and crystalline KCl. The Brillouin peaks in both molten salts are very sharp with linewidths only slightly larger than the values expected due to shear viscosity alone. Sound velocities determined from the Brillouin shifts are in excellent agreement with ultrasonic values and with a previous Brillouin scattering experiment on molten KCl. In experiments with progressively larger free spectral ranges (FSR) from 0.178 to 20 cm^{-1}, no evidence for any Rayleigh wing spectrum was found in either melt. A flat, highly depolarized background was observed in triple-pass experiments on CsCl at 20 cm^{-1} FSR, indicating that the broad depolarized collision-induced spectrum observed in Raman scattering experiments extends down to zero frequency. The limiting $\omega \rightarrow 0$ differential cross section deduced from the background in our spectra agrees to within a factor of 1.4 with the value 2.29×10^{-8}/(cm sr cm^{-1}) obtained from Raman experiments by Mitchell and Raptis.

I. INTRODUCTION

During the past 15 years, understanding of the structure of fluids has been greatly advanced by experimental and computer simulation studies of the simple monatomic rare-gas fluids. Recently, a number of studies have been directed towards elucidating the structure of molten salts, particularly the alkali halides which represent the next level of complexity beyond the simple monatomic fluids. Neutron scattering studies of several isotopically substituted molten alkali halides have provided extensive data on the partial radial distribution functions which have been found to be in reasonable agreement with molecular dynamics simulations.[1,2] The neutron scattering experiments have also shown that molten salts possess local structural ordering over regions of about 25 Å involving charge ordering over about five coordination shells. These ordered regions should have short lifetimes due to the high ionic diffusion rates in molten salts.[3]

Raman scattering experiments on argon, krypton, and neon revealed a broad depolarized spectrum caused by transient interactions between atoms which modify the atomic polarizability. Studies of this collision-induced (or intermolecular) depolarized light scattering in argon at low densities revealed an exponential dependence of intensity on frequency: $I_{VH} = I_0 e^{-\omega/\Delta}$ with $\Delta \approx 10$ cm^{-1} at low densities increasing to ≈ 40 cm^{-1} at the triple-point density $\rho_{tp} = 800$ amagats. At higher densities, the spectrum exhibits two regions of exponential form. Below $\omega_0 \approx 50$ cm^{-1}, $I_{VH} = I_0 e^{-\omega/\Delta_1}$, and above ω_0, $I_{VH} = I_0 e^{-\omega/\Delta_2}$. With increasing density above ρ_{tp}, Δ_2 increases while Δ_1 decreases, so a plot of $\ln I_{VH}$ versus ω exhibits two straight-line segments meeting at $\omega_0 \approx 50$ cm^{-1}, with a smaller slope for the high-frequency segment. For neon, on the contrary, $\Delta_2 < \Delta_1$, so the high-frequency segment has a larger slope.[4–6] These Raman spectra have been explained, at least in part, by a combination of short-range interaction-induced electron overlap at high frequencies, and dipole-induced-dipole longer-range interactions at low frequencies.[6,7]

Raman scattering studies of molten alkali halides were recently reported by Mitchell and Raptis,[8] by Giergiel, Subbaswamy, and Eklund[9] and by Raptis *et al.*[10] with substantially equivalent results. Both polarized and depolarized spectra exhibit a high-frequency exponential segment and a low-frequency nearly exponential segment. There is, however, a "shoulder" separating these two regions which has been attributed to the residue of the optical vibrational mode in the solid.[8,10] Such optic modes have been predicted to occur in molten alkali halides both from theoretical calculations and computer simulations, and an LO mode has been observed by neutron scattering in RbCl.[11] Another noteworthy feature observed in the light scattering work is that the proportion of *depolarized* scattering increases rapidly with decreasing frequency.

These Raman scattering experiments raised several interesting questions that suggest extending the measurements to lower frequencies: (1) Does the intensity observed in the Raman experiments continue to rise with decreasing frequency all the way to $\omega=0$? (2) Is there additional low-frequency (Rayleigh wing) structure associated with relaxation of the local ordering or with rotational motion of the transient clusters? (3) Does the low-frequency spectrum exhibit sharp, well-defined Brillouin components, or are they broadened by relaxation processes, contributing some of the intensity seen in the low-frequency part of the Raman spectra? (4) How does the low-frequency spectrum differ between the crystal and the melt? (5) What is the depolarization ratio of the Brillouin and other low-frequency components?

In order to explore these questions, we have undertaken a Brillouin scattering study of molten CsCl and of crystalline and molten KCl. The experiments are described in Sec. II, the results are presented and analyzed in Sec. III, and our conclusions are given in Sec. IV.

II. EXPERIMENTS

Brillouin scattering studies of molten salts have been reported previously by Reinsborough and Valleau[12] for $AgNO_3$ and $Ca(NO_3)_2\cdot 4H_2O$, by Gustafsson, Gunilla Knape, and Torell[13] for $NaNO_3$ and KNO_3, and by Torell and Gunilla Knape[14] for NaCl and KCl. These were low-resolution experiments, designed to determine hypersonic velocities from the Brillouin shifts.

Our measurements were performed with a high-resolution computer-controlled interferometer (Tropel model 350) in either single- or triple-pass, and a single-mode argon laser (Spectra-Physics model 165) operating at 5145 Å. Data were collected in a Digital Equipment Corporation PDP8E minicomputer, which also maintained interferometer alignment, and transferred to a central Digital Equipment Corporation PDP10 computer for subsequent analysis by a nonlinear least-squares-fitting program. (The apparatus has been described in detail in a previous publication.[15])

Samples were mounted in an optical furnace specially designed for spectroscopy of molten salts and hot solids.[16] The sample was loaded into a 1-cm-square silica cell which was fused to a silica tube which extends through the top of the oven and was evacuated and backfilled with inert buffer gas to inhibit sublimation. The main space inside the furnace was evacuated with a diffusion pump and operated under vacuum at all times. Three optical windows in the midplane allowed 90° scattering in a horizontal scattering plane. Temperature was determined by a chromel-alumel thermocouple placed in contact with the bottom of the cell, measured by an Omega model 2175A digital thermometer. Readings were corrected so that T_m of KCl=770 °C.

A. CsCl

99.9% pure CsCl powder (Analar Analytical Reagent, BDH Chemicals Ltd.) was loaded in a silica cell and thoroughly dried by pumping for one day at room temperature followed by 400 °C overnight. The optical cell was then backfilled with Argon gas to one atmosphere and gradually heated through the melting temperature. Brillouin spectra were collected with mirror separations of 28.1, 10.1, 7.5, and 0.25 mm [free spectral range (FSR) of 0.178, 0.5, 0.67, and 20 cm^{-1}] in single pass and a separation of 0.25 mm in triple pass.

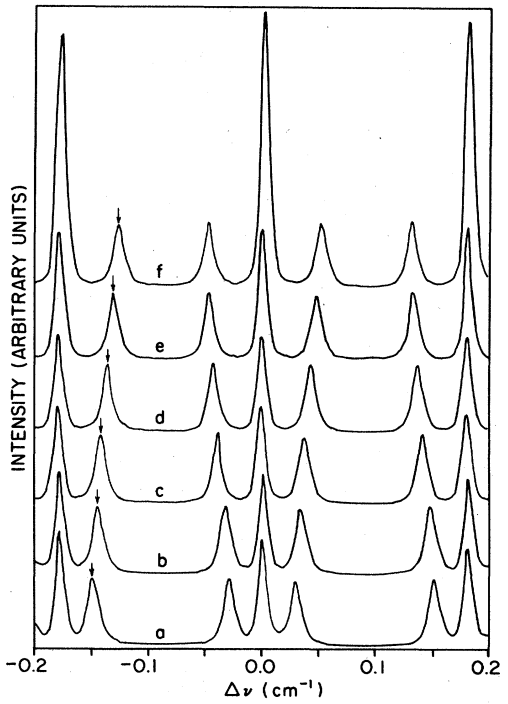

FIG. 1. *VT* Brillouin spectra of molten CsCl. FSR of 0.178 cm^{-1}. *a*, $T=659$ °C; *b*, $T=697$ °C; *c*, $T=750$ °C; *d*, $T=801$ °C; *e*, $T=849$ °C; and *f*, $T=879$ °C. The arrows indicate the Stokes Brillouin component associated with the central Rayleigh line. The spectra are normalized for uniform Brillouin peak height.

A series of CsCl single-pass Brillouin spectra in *VT* polarization is shown in Fig. 1 with a FSR of 0.178 cm^{-1}. Temperatures range from 659 °C (bottom) to 879 °C (top). These spectra were analyzed by a nonlinear least-squares-fitting program which fits the Rayleigh lines to a Voigt function, establishing the instrumental transmission function $T(\omega)$. Each Brillouin component is assumed to be Lorentzian, characterized by a center frequency ν_B and full width at half maximum $\Delta\nu_B$. A set of trial Lorentzians is convoluted with the instrument function, and the center frequencies and linewidths are varied to obtain a best fit to the entire spectrum. In the single-pass experiment, the average working finesse was 27 giving an instrumental linewidth of 0.007 cm^{-1}. The observed Brillouin linewidths were typically about 0.01 cm^{-1}, and after deconvolution fell in the range 0.003 to 0.005 cm^{-1} with no clear temperature dependence. The Brillouin shift, hypersonic velocity, and full width at half maximum deduced from these spectra are plotted in Fig. 2 and listed in Table I together with the refractive index given by Iwadate *et al.*[17] The viscosities given in the last three

TABLE I. Results of Brillouin scattering measurements on molten CsCl.

Spectrum number (see Fig. 1)	T (°C)	ν_B (cm^{-1})	n[a]	q (cm^{-1})	Sound velocity C_S (cm/sec) Brillouin	Ultrasonic[b]	$\Delta\nu_B$ (cm^{-1}) (FWHM)	η_e (poise)	η_s (poise)	η_b[b] (poise)
1 (curve *a*)	659	0.148	1.461	2.52×10^5	1.11×10^5	1.15×10^5	0.0038	0.023	0.017	0.32
2 (curve *b*)	697	0.145	1.455	2.51×10^5	1.09×10^5	1.13×10^5	0.0032	0.020	0.015	0.32
3 (curve *c*)	750	0.139	1.446	2.48×10^5	1.06×10^5	1.09×10^5	0.0032	0.020	0.013	0.32
4 (curve *d*)	801	0.135	1.438	2.48×10^5	1.03×10^5	1.06×10^5	0.0044	0.026	0.010	0.32
5 (curve *e*)	849	0.131	1.430	2.47×10^5	1.00×10^5	1.02×10^5	0.0034	0.020	0.008	0.32
6	878	0.129	1.425	2.46×10^5	0.99×10^5	1.00×10^5	0.0044	0.026	0.007	0.32
7 (curve *f*)	879	0.129	1.425	2.46×10^5	0.99×10^5	1.00×10^5	0.0050	0.030	0.007	0.32

[a]Reference 17.
[b]Reference 19, pp. 251 and 258.

columns of Table I will be discussed in the next section.

The integrated Brillouin intensity [see Fig. 2(d)] was found to increase with increasing temperature up to 800 °C. Above this temperature, some contamination of the windows occurred causing the apparent Brillouin intensity to decrease.

No evidence of a Rayleigh wing was seen in the spectra of Fig. 1, or in the depolarized spectra taken with the same 0.178-cm^{-1} FSR. The mirror separation was gradually decreased and spectra were collected at $d=10.1$ mm, 7.5 mm and finally at a minimum $d=0.25$ mm, giving a maximum FSR of 20 cm^{-1}. With this maximum FSR, some indication of a Rayleigh wing was seen in single pass, but not in triple pass, showing that the single-pass wing was just the skirt of the instrument transmission function.

A triple-pass *HT* CsCl spectrum at $T=672$ °C is shown in Fig. 3. The background spectrum obtained with the laser beam blocked is also shown, indicating the background level due to thermal radiation from the oven and dark current in the phototube. This background signal is about 50 counts/sec. There is clearly an additional frequency-independent signal present at about 22 counts/sec. The *VT* spectrum shows a similar frequency-independent signal, indicating that $I_{VV}\approx I_{HH}\approx 11$ counts/sec, and that the depolarization I_{HH}/I_{VV} is essentially complete ($\sim 75\%$).

In the *VT* spectrum, the large central component was both bigger and broader than in the *HT* spectrum since it contains the Rayleigh and Brillouin components. The Brillouin components disappeared in *HT* polarization, indicating that they are 100% polarized. The Rayleigh

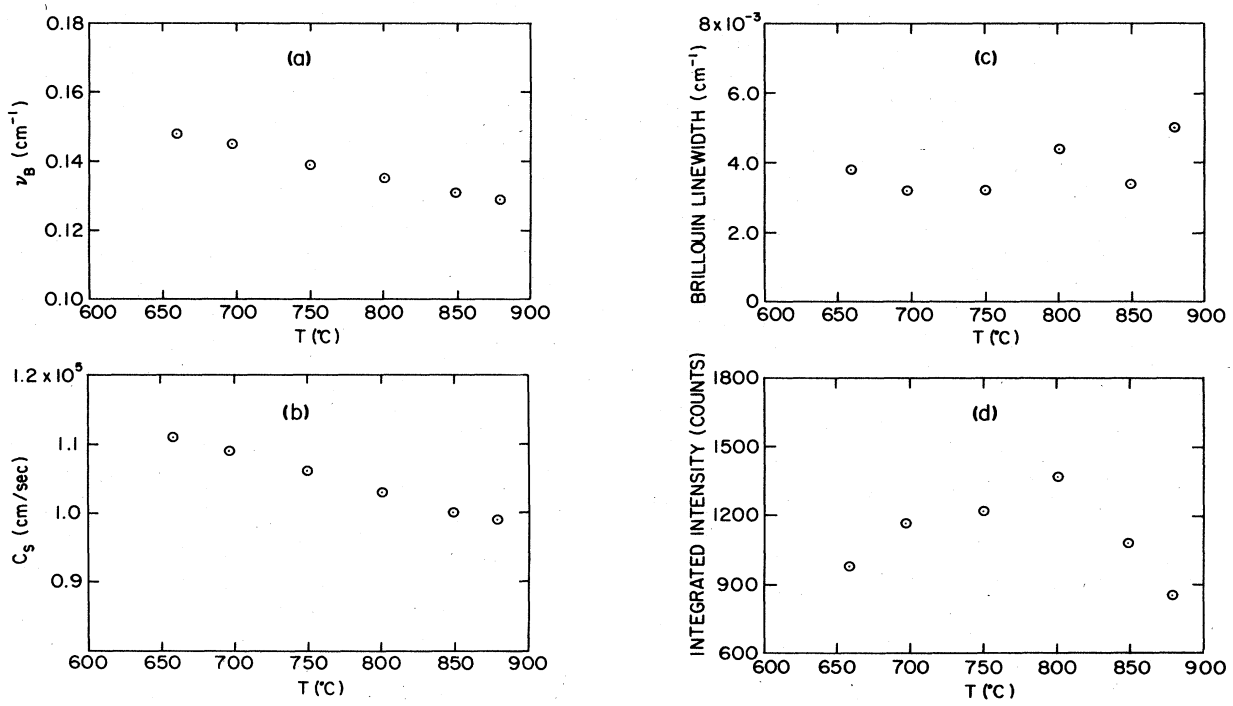

FIG. 2. Temperature dependence of properties of molten CsCl deduced from the Brillouin spectra. (a) Brillouin shift, (b) sound velocity c_s, (c) Brillouin linewidth, (d) integrated intensity of Brillouin lines.

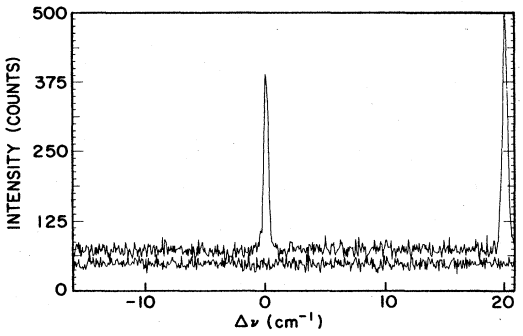

FIG. 3. Triple-pass *HT* spectrum of CsCl with a FSR of 20 cm^{-1}. The background signal recorded with the laser beam blocked is also shown.

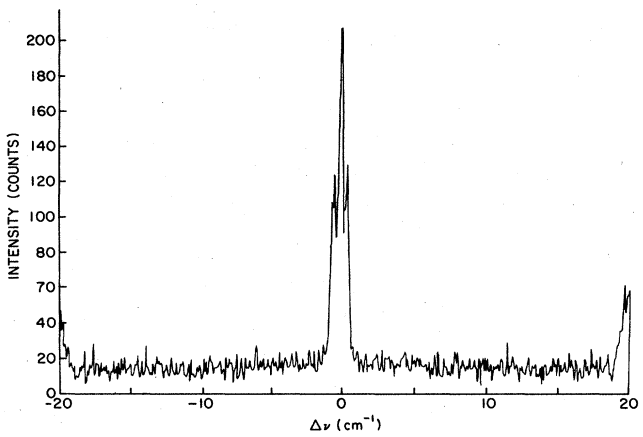

FIG. 4. Triple-pass *VT* spectrum of benzene recorded under the same conditions as the CsCl spectrum of Fig. 3.

component, on the contrary, was always present in *HT* polarization, indicating partial depolarization. The inferred depolarization ratio was not repeatable, however, and from this and other tests we concluded that part of the observed Rayleigh intensity in both polarizations, particularly for the KCl crystal spectra, resulted from multiple elastic scattering of laser light inside the oven. The observed depolarization of the Rayleigh line was therefore assumed not to be significant. A *VT* benzene spectrum, recorded under the same conditions as the spectrum of Fig. 3, is shown in Fig. 4. This served as a calibration for determining the differential cross section for CsCl, as described in the next section.

B. KCl

(100) cubes having edges of approximately 1 cm were cleaved from a large KCl single crystal grown under conditions free of oxygen containing impurities, generously provided by Dr. Philipp H. Klein of the Naval Research Laboratory. The crystal was placed in the optical cell, heated to 400 °C under vacuum and backfilled with argon at 1 atm. Brillouin spectra with $\mathbf{q}\|[110]$ were collected at temperatures from room temperature up to 896 °C in single pass with mirror separations of 17.1, 11.2, 7.5, and 0.25 mm.

In Fig. 5, three KCl Brillouin spectra are shown for $d=7.5$ mm (a FSR of 0.667 cm^{-1}). The lower two spectra ($T=707$ and 770 °C) are in the crystal, while the upper spectrum ($T=810$ °C) is in the melt. The middle spectrum was recorded as the crystal was beginning to melt, but no special features associated with premelting were observed in the Brillouin spectra. The crystal spectra exhibit strong LA modes in *VT* polarization, but no Brillouin components in *HT* polarization. Although TA scattering is allowed in *HT* polarization for this geometry, it is expected to be quite weak. Note that the Rayleigh intensities ($\approx$7000 counts/sec) are approximately equal in all three spectra, while the Brillouin components are about ten times stronger in the melt than in the crystal.

The Brillouin shifts, intensities, linewidths, sound velocities, and effective viscosities deduced from the KCl experiments are listed in Table II and plotted in Fig. 6. Analysis of higher-resolution data obtained with $d=17.1$ mm gave very similar results.

III. ANALYSIS OF RESULTS

A. Sound velocities

The sound velocity c_s is related to the Brillouin shift ν_B (in cm^{-1}) by $c_s q=\omega=2\pi c\nu_B$, where

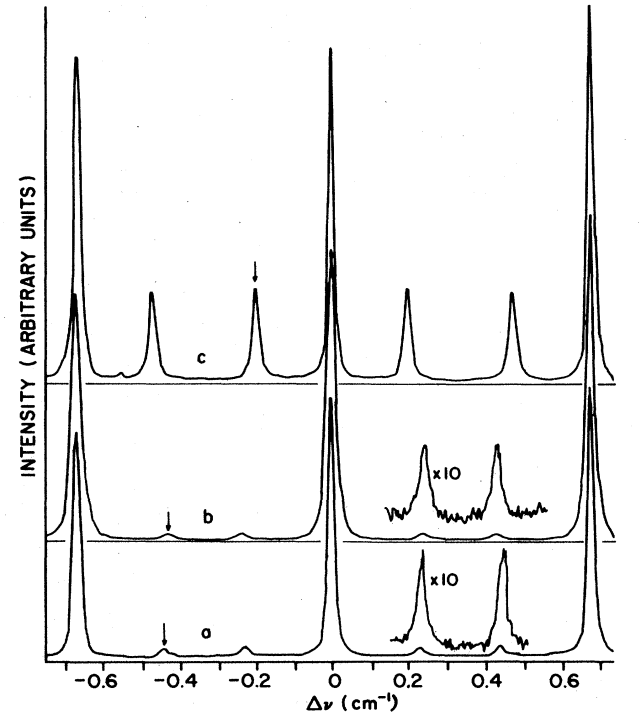

FIG. 5. *VT* Brillouin spectra of crystalline (a,b) and molten (c) KCl. FSR of 0.667 cm^{-1}. a, $T=707$ °C; b, $T=770$ °C; and c, $T=810$ °C. The Rayleigh peaks are approximately 7000 counts/sec in all three spectra. The arrows indicate the Stokes LA Brillouin component associated with the central Rayleigh line.

TABLE II. Results of Brillouin scattering measurements on KCl.

(a) Melt

Spectrum number	T (°C)	ν_B (cm^{-1})	n	q (cm^{-1})	Sound velocity C_S (cm/sec) Brillouin	Ultrasonic	$\Delta\nu_B$ (cm^{-1}) (FWHM)	η_e (poise)	η_s (poise)	η_b (poise)
1	775	0.202	1.404	2.43×10^5	1.57×10^5	1.60×10^5	0.0059	0.022	0.015	0.26
2	788	0.201	1.402	2.42×10^5	1.57×10^5	1.59×10^5	0.0053	0.019	0.015	0.25
3	810	0.198	1.398	2.42×10^5	1.54×10^5	1.57×10^5	0.0055	0.020	0.014	0.24
4	863	0.192	1.389	2.40×10^5	1.51×10^5	1.53×10^5	0.0055	0.020	0.012	0.22
5	896	0.188	1.383	2.39×10^5	1.48×10^5	1.50×10^5			0.011	0.20

(b) Crystal

Spectrum number	T (°C)	ν_B (cm^{-1})	n	q (cm^{-1})	Sound velocity C_S (cm/sec) Brillouin	$\Delta\nu_B$ (cm^{-1}) (FWHM)
6	417	0.478	1.495	2.58×10^5	3.49×10^5	0.0157
7	499	0.466			3.40×10^5	0.0149
8	618	0.450			3.29×10^5	0.0130
9	708	0.437			3.19×10^5	0.0108
10	731	0.433			3.16×10^5	0.0095
11	749	0.431			3.15×10^5	0.0107
12	762	0.429			3.13×10^5	0.0106
13	770	0.427			3.12×10^5	0.0094

$q=(4\pi n/\lambda)\sin(\theta/2)$. For $\theta=90°$ and $\lambda=5145$ Å, $q=1.727\times10^5 n$ cm^{-1}. In Tables I and II(a) the refractive index n of molten CsCl and KCl was computed from the six-parameter formula of Iwadate, Mochinaga, and Kawamura.[17] For the KCl crystal data of Table II(b), we used the room-temperature value[18] of $n=1.495$ since no temperature-dependent values were available. We note that our values of c_s for both molten CsCl and KCl are in

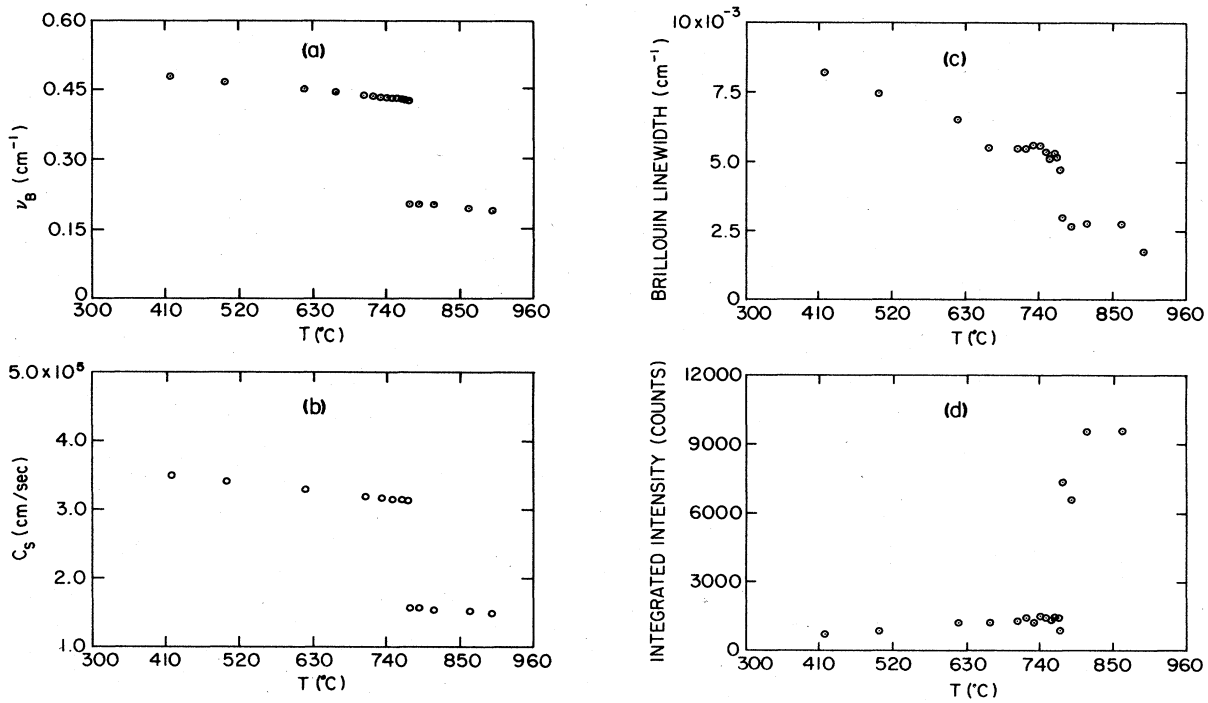

FIG. 6. Temperature dependence of KCl properties deduced from the Brillouin spectra. (a) Brillouin shift, (b) sound velocity c_s, (c) Brillouin linewidth, (d) integrated intensity of Brillouin lines.

good agreement with the ultrasonic values[19] and that our values for molten KCl agree to within 1% with the results of Torell and Gunilla Knape who measured n independently.

B. Brillouin linewidths

The full width at half maximum (FWHM) of a Brillouin component of a fluid is given by[6]

$$\Delta\omega_B = 2\pi c \Delta\nu_B = \frac{1}{\rho}\left[\tfrac{4}{3}\eta_s + \eta_b + \Lambda\left(\frac{1}{C_v} - \frac{1}{C_p}\right)\right] q^2 = \frac{\tfrac{4}{3}\eta_e q^2}{\rho}\,, \tag{1}$$

where $\Delta\nu_B$ is the FWHM in cm^{-1} of the Brillouin component, η_s and η_b are the shear and bulk viscosities, Λ is the thermal conductivity, ρ is the density, and C_v and C_p are the specific heats at constant volume and pressure, respectively. The second (η_B) term in Eq. (1) represents attenuation due to internal degrees of freedom of the melt, while the third term represents attenuation due to heat transport between high- and low-pressure regions in the adiabatic sound wave. The "effective viscosity" η_e is defined by Eq. (1) and the quantity $(\eta_e - \eta_s)$ is a measure of the importance of the last two terms.

An estimate of the heat-transport term based on data in Janz[19] indicates that its contribution to the linewidth should be about 20% of the contribution from the shear viscosity term. Thus, referring to the η_e and η_s columns in Table I, we see that the first and third terms in Eq. (1) account for most of the observed Brillouin linewidth, ranging from about 90% for $T \leq 750$°C to 50% for $T \geq 750$°C but in all cases η_e is considerably less than all the low-frequency (ultrasonic) values of η_B shown in the table.

C. Analysis of background

Since no Rayleigh-wing features were seen as the FSR was increased from 0.178 to 20 cm^{-1}, we conclude that the only low-frequency scattering (apart from the Rayleigh and Brillouin components) comes from the broad vibrational spectra observed in the Raman experiments. We therefore attempted to compare the differential cross section at $\omega \to 0$ deduced from the flat background in our experiments with the value obtained by Mitchell and Raptis[8] by extrapolating the data in their Fig. 2 to $\omega = 0$.

Mitchell and Raptis[8] found the integrated polarized Raman cross section for CsCl at 670 °C as 4.61×10^{-29} cm^2/ion pair steradian by comparing the observed intensity with the 992 cm^{-1} Raman line of benzene. Since for CsCl at this temperature there are 9.32×10^{21} ion pairs per cm^3, the integrated cross section per unit volume is $(1/V)(d\sigma/d\Omega) = 4.31 \times 10^{-7}$/cm sr.

The $\omega \to 0$ limit of the *differential* cross section can also be found from these data. Since the extrapolated intercept is 8.13×10^5 counts/sec cm^{-1} while the integrated count rate under the curve is 1.525×10^7 counts/sec, the Mitchell-Raptis result is

$$\left[\frac{1}{V}\frac{d^2\sigma}{d\Omega\, d\omega}\right]_{\omega\to 0} = \frac{8.13\times 10^5}{1.525\times 10^7}\,\frac{1}{V}\,\frac{d\sigma}{d\Omega} = 2.29\times 10^{-8}/(\mathrm{cm\ sr\ cm}^{-1})\,. \tag{2}$$

Our estimate of the $\omega \to 0$ limit of the differential cross section was derived from the flat background in the CsCl spectrum of Fig. 3, calibrated against the benzene spectrum of Fig. 4 by the procedure outlined in the Appendix. From the present measurements, we find for molten CsCl that the differential cross section for $\omega \to 0$ is

$$\left[\frac{1}{V}\frac{d^2\sigma}{d\Omega\, d\omega}\right]_{\omega\to 0} = 1.79\times 10^{-8}/(\mathrm{cm\ sr\ cm}^{-1})\,.$$

This is 0.78 of the value given above derived from the value extrapolated from the data of Mitchell and Raptis.

IV. DISCUSSION

We first discuss the light-scattering observations themselves, their relation to other light-scattering work, and the factors required for their occurrence. Secondly we comment on these factors from the point of view of the dynamics of the molten salts.

A. Light scattering

The present experiments have extended the range of wave-number transfer to 10^{-2} cm^{-1}, in fact covering the region up to 10 cm^{-1}, thereby overlapping the lowest $\bar{\nu}$ of 4 cm^{-1} in previously reported Raman experiments. The significant "light scattering" facts seem to be as follows.

(a) The intensities observed for the underlying spectra are in good agreement with those determined in the Raman type of experiment.

(b) The high depolarization ratios observed in the lower $\bar{\nu}$ range of the Raman work are seen in the present work to continue to very low $\bar{\nu}$.

(c) The Brillouin lines appear to be superimposed on this broader spectrum, but the lines themselves are, in contrast to the background, highly polarized. Clearly there must be more than one process involved.

(d) We have not observed a significant Rayleigh-wing component. Furthermore, if such a component had been present the agreement between the independent sets of intensity data would not have been found.

(e) The Brillouin lines are surprisingly strong and narrow. They are about an order of magnitude stronger than those observed in the hot crystals and show FWHM less by about a factor of 3.

(f) The position of the lines correspond to sound velocities smaller by a factor of about 2 than in the corresponding crystal.

(g) In detail the values in (f) may be understood from the magnitudes of independently measured related properties. Although there is a density change from 1.984 $\mathrm{g\,cm}^{-3}$ in crystalline KCl to 1.51 in the melt, the major contribution to the velocity difference comes from the elastic constants. For the crystal we have measured

$v_{110}=(1/2\rho)(C_{11}+C_{12}+4C_{44})^{1/2}$. Calculating this using published values for the elastic constants gives a value of 3.84×10^5 cm^{-1}, which is precisely the value determined at room temperature measured in these experiments.

For the isotropic melt the velocity is given by $(1/\rho K)^{1/2}$, where K is the adiabatic compressibility of the melt ($K=26.6\times10^{-12}$ cm^2/dyn) giving a velocity of 1.58×10^5 compared with the measured value of 1.57×10^5 cm sec^{-1}.

(h) Conversely we can use the measured Brillouin shifts to obtain accurate values of the compressibilities of the melts using

$$K=-\frac{1}{v}\left[\frac{\partial v}{\partial p}\right]_T=q^2/4\pi^2\bar{\nu}^2c^2\rho\ ,$$

where q (cm^{-1}) is the magnitude of the wave vector, c (cm sec^{-1}) the velocity of light and ρ (g cm^{-3}) is the density. We find at the melting temperatures, $K=26.9\times10^{-12}$ cm^2 dyn^{-1} for molten KCl and 30.8×10^{-12} cm^{2}dyn^{-1} for molten CsCl. These values are to be compared with the 26.6 and 28.7 determined for the 26.6 and 28.7 determined for them ultrasonically.

(i) The widths of the Brillouin lines in the melts are considerably less than those calculated using values of the bulk viscosities determined from ultrasonic measurements. We conclude that at the higher frequencies of the light-scattering experiments, the bulk viscosities in the melt are lower by at least an order of magnitude than those measured ultrasonically. The values which we have used for the shear viscosities in this calculation were taken from Janz,[19] but they were in fact measured by Lorentz[20] in 1912. There must be doubt about their reliability, but any conceivable inaccuracy could not affect the above conclusion.

B. Molten salts

As expected, the measurements show characteristics of molten salts that were known from other observations —notably that the compressibilities in the molten state are greater than in the crystal by a factor of about 5. A larger compressibility means a weak repulsive potential which is consistent with the substantial decrease in density.

The breadth of Brillouin lines in a crystal is determined by anharmonic coupling to other vibrational modes. To the extent that there is a smaller spread of frequencies of modes at a given q in the melt, because of its isotropy than in the anisotropic crystal, this contribution to the breadth would be less.

In addition to these macroscopic properties of the melts, we know from work already cited[1,2] that short-range order occurs over diameters of about 25 Å. It has also been found by McGreevy and Mitchell[11] and McGreevy *et al.*[3,21] that there are vibrational modes associated with this ordering. The lifetime of the order in a particular spatial location is clearly affected by the diffusive motions which dominate the quasielastic neutron scattering. However there has been no experimental information on the possibility that "globular" motions—slow rotations, librations or structural relaxations—could be contributing to the spatial fluctuations of the local order. Such effects have been observed in molecular liquids for example by Starunov *et al.*[22] but they are clearly not present in our observations. We conclude that such processes are not important in the molten salts examined, a conclusion which favors a fluctuating continuous structure exhibiting short-range order, rather than a quasimolecular structure.

ACKNOWLEDGMENTS

We wish to thank Dr. R. L. McGreevy, Professor J. L. Birman and Professor R. J. Elliott for helpful discussions, and Dr. Philip Klein for providing the high quality KCl crystal used in this experiment. Support for this research was provided by the U.S. Department of Energy and the Science and Engineering Research Council (SERC) of the United Kingdom. Travel funds were provided by the North Atlantic Treaty Organization (NATO) Scientific Affairs Division through a NATO grant for collaborative research.

APPENDIX

We can estimate the $\omega\to0$ limit of the differential cross section from the flat background in the CsCl spectrum of Fig. 3, calibrated against the benzene spectrum of Fig. 4 by the following procedure. The intensity of light transmitted through a Fabry-Perot interferometer with mirror separation d when the incident light has a spectrum $S(\omega)$ is

$$I=\sum_m\int_\omega T(\omega-\omega_m)S(\omega)d\omega\ , \tag{A1}$$

where $\omega_m=m(c/2d)$ is the center frequency of the mth transmission maximum (or *FP* mode) and $T(\omega-\omega_m)$ is the transmission function for that mode.

If $S(\omega)$ is a slowly varying function of ω, then inside the integral $S(\omega)=S(\omega_m)$, whence

$$I=\sum_m\int_\omega T(\omega-\omega_m)S(\omega_m)d\omega=T_{\rm int}\sum_m S(\omega_m)\ , \tag{A2}$$

where

$$T_{\rm int}=\int_\omega T(\omega-\omega_m)d\omega$$

is the integrated transmission function for a single *FP* mode which is independent of ω_m. Also, we can write

$$S(\omega)=B\left[\frac{d^2\sigma}{d\Omega\,d\omega}\right]_{\omega_m}F(\omega)\ ,$$

where B is a constant which is proportional to the laser power, the scattering volume, the collection solid angle, the photomultiplier quantum efficiency and the throughput of the collection optics, and $F(\omega)$ is the transmission function of the narrow-band filter located in front of the photomultiplier relative to its value at 5145 Å. Letting

$$\left[\frac{d^2\sigma}{d\Omega\,d\omega}\right]_{\omega_m}=R(\omega_m)\left[\frac{d^2\sigma}{d\Omega\,d\omega}\right]_{\omega\to0}\ ,$$

we have

$$I=BT_{\rm int}\left[\frac{d^2\sigma}{d\Omega\,d\omega}\right]_{\omega\to0}\sum_m R(\omega_m)F(\omega_m)\ . \tag{A3}$$

Values of $R(\omega_m)$ were obtained by dividing the intensities shown in Fig. 2 of Ref. 8 by the extrapolated $\omega \rightarrow 0$ intercept of 8.13×10^5. Values of $F(\omega_m)$ were found by measuring the filter transmission directly. The sum $\sum_m R(\omega_m)F(\omega_m)$ was computed by successively adding values for pairs of modes at ± 20 cm^{-1}, ± 40 cm^{-1}, etc. to the value 1.0 for the central mode. The sum converged to approximately 2.1. The observed intensity I was 11 counts/sec.

The quantity BT_{int} was obtained from a benzene Brillouin spectrum obtained under the same conditions as the CsCl spectrum. For a spectrum $S(\omega)$ confined to a frequency region much narrower than the FSR, Eq. (A1) simplifies to

$$I=\int_\omega T(\omega-\omega_m)S(\omega)d\omega \ .$$

If ω_m is scanned by scanning d, and the observed spectrum is integrated, then

$$\int_{\omega_m} I(\omega_m)d\omega_m=\int_\omega\int_{\omega_m} T(\omega-\omega_m)S(\omega)d\omega\, d\omega_m$$
$$=T_{\text{int}}\int_\omega S(\omega)d\omega=T_{\text{int}}B\frac{1}{V}\frac{d\sigma}{d\Omega} \ .$$

The theoretical integrated Rayleigh-Brillouin cross section is given by

$$\left[\frac{1}{V}\frac{d\sigma}{d\Omega}\right]=\frac{r^2I_s}{VI_0}=\frac{\pi^2}{\lambda^4}(\epsilon-1)^2kT\kappa_T \ ,$$

where κ_T is the isothermal compressibility. For benzene with $\lambda=5145$ Å, this gives[23]

$$(1/V)(d\sigma/d\Omega)=8.72\times10^{-6}/\text{cm} \ .$$

Using the digital data of Fig. 4, the integrated count rate was found to be 2549 counts/sec. Therefore, $2549=T_{\text{int}}B8.72\times10^{-6}$, so $BT_{\text{int}}=2.92\times10^8$. With this value, Eq. (A3), for the CsCl $\omega\rightarrow0$ differential cross section, becomes

$$(d^2\sigma/d\Omega\, d\omega)_{\omega\rightarrow0}=11/2.1\times2.92\times10^8$$
$$=1.79\times10^{-8}/(\text{cm sr cm}^{-1}) \ ,$$

which is 0.78 times the Mitchell-Raptis result, in agreement well within the errors introduced by the approximations made in this calculation.

[1]E. W. J. Mitchell, P. F. J. Poncet, and R. J. Stewart, Philos. Mag. **34**, 721 (1976).

[2]J. Locke, R. L. McGreevy, S. Messoloras, E. W. J. Mitchell, and R. J. Stewart, Philos. Mag. (to be published).

[3]R. L. McGreevy, E. W. J. Mitchell, and F. M. A. Margaca, J. Phys. C **17**, 775 (1983), and references cited therein.

[4]P. A. Fleury, W. B. Daniels, and J. M. Worlock, Phys. Rev. Lett. **27**, 1493 (1971).

[5]P. A. Fleury and J. P. Boon, Adv. Chem. Phys. **24**, 1 (1974).

[6]B. J. Berne and R. Pecora, *Dynamic Light Scattering* (Wiley, New York, 1976).

[7]W. M. Gelbart, Adv. Chem. Phys. **26**, 1 (1974).

[8]E. W. J. Mitchell and C. Raptis, J. Phys. C **16**, 2973 (1983).

[9]J. Giergiel, K. R. Subbaswamy, and P. C. Eklund, Phys. Rev. B **29**, 3490 (1984).

[10]C. Raptis, E. W. J. Mitchell, and R. A. J. Bunten, J. Phys. C **16**, 5351 (1983).

[11]R. L. McGreevy and E. W. J. Mitchell, J. Phys. C **15L**, 1001 (1982).

[12]V. C. Reinsborough and J. P. Valleau, Can. J. Chem. **50**, 2704 (1972).

[13]S. E. Gustafsson, H. E. Gunilla Knape, and L. M. Torell, Z. Naturforsch. **29a**, 469 (1974).

[14]L. M. Torell and H. E. Gunilla Knape, Z. Naturforsch. **34a**, 899 (1979).

[15]W. Yao, H. Z. Cummins, and R. H. Bruce, Phys. Rev. B **24**, 424 (1981).

[16]C. Raptis, J. Phys. E **16**, 749 (1983).

[17]Y. Iwadate, J. Mochinaga, and K. Kawamura, J. Phys. Chem. **85**, 3708 (1981).

[18]*American Institute of Physics Handbook*, 2nd ed., edited by D. E. Gray (McGraw-Hill, New York, 1963), pp. 6—31.

[19]G. J. Janz, *Molten Salts Handbook* (Academic, New York, 1967).

[20]R. Lorentz, Z. Phys. Chem. Stoechiom. Verwandshaftsl. **79**, 63 (1912).

[21]F. M. A. Margaca, R. L. McGreevy, and E. W. J. Mitchell, J. Phys. C **17**, 4725 (1984).

[22]V. S. Starunov, E. V. Tiganov, and I. L. Fabelinskii, ZhETF Pis'ma **4**, 262 (1966) [JETP Lett. **4**, 176 (1966)].

[23]H. Z. Cummins and R. W. Gammon, J. Chem. Phys. **44**, 2785 (1966).